Accepted Article

PROF. MALCOLM BENNETT (Orcid ID : 0000-0003-0475-390X)
PROF. PETER HEDDEN (Orcid ID : 0000-0002-4216-7488)

Article type : Regular Manuscript

Short Title: GA biosynthesis in the root tip

Full Title Mapping sites of gibberellin biosynthesis in the Arabidopsis root tip

Authors: Richard Barker[1,2], Maria Nieves Fernandez Garcia[3], Stephen J. Powers[1], Simon Vaughan[1], Malcolm J. Bennett[2], Andrew L. Phillips[1], Stephen G. Thomas[1] and Peter Hedden[1,4].

[1]Rothamsted Research, Harpenden, Hertfordshire AL5 2JQ, UK; [2]Plant & Crop Sciences, School of Biosciences, University of Nottingham, Sutton Bonington LE12 5RD, UK; [3]Department of Abiotic Stress and Plant Pathology, Centro de Edafología y Biología Aplicada del Segura (CSIC), Murcia, Spain; [4]Laboratory of Growth Regulators, Centre of the Region Haná for Biotechnological and Agricultural Research, Institute of Experimental Botany, Czech Academy of Sciences, and Faculty of Science, Palacký University, CZ-783 71 Olomouc, Czech Republic

Richard Barker https://orcid.org/0000-0002-9951-1382
Maria Nieves Fernandez Garcia https://orcid.org/0000-0002-5860-2173
Stephen J. Powers https://orcid.org/0000-0003-3349-4425
Simon Vaughan https://orcid.org/0000-0002-1550-6915
Malcolm J. Bennett https://orcid.org/0000-0003-0475-390X
Andrew L. Phillips https://orcid.org/0000-0002-6406-7015
Stephen G. Thomas https://orcid.org/0000-0001-6731-2699
Peter Hedden https://orcid.org/0000-0002-4216-7488

This article has been accepted for publication and undergone full peer review but has not been through the copyediting, typesetting, pagination and proofreading process, which may lead to differences between this version and the Version of Record. Please cite this article as doi: 10.1111/NPH.16967

This article is protected by copyright. All rights reserved

Accepted Article

Author for correspondence:

Peter Hedden

Tel: +44 1582938133

Email: peter.hedden@rothamsted.ac.uk

Received: *6 July 2020*
Accepted: *5 September 2020*

Summary

- Root elongation depends on the action of the gibberellin (GA) growth hormones, which promote cell production in the root meristem and cell expansion in the elongation zone. Sites of GA biosynthesis in the roots of 7 day-old *Arabidopsis thaliana* seedlings were investigated using tissue-specific GA inactivation in wild type (Col-0) or rescue of GA-deficient dwarf mutants.
- Tissue specific GA-depletion was achieved by ectopic expression of the GA-inactivating enzyme AtGA2ox2, which is specific for C_{19}-GAs, and AtGA2ox7, which acts on C_{20}-GA precursors. In addition, tissue-specific rescue of *ga20ox* triple and *ga3ox* double mutants was shown. Furthermore, GUS reporter lines for major *GA20ox, GA3ox* and *GA2ox* genes were used to observe their expression domains in the root.
- The effects of expressing these constructs on the lengths of the root apical meristem and cortical cells in the elongation zone confirmed that roots are autonomous for GA biosynthesis, which occurs in multiple tissues, with the endodermis a major site of synthesis.
- The results are consistent with the early stages of GA biosynthesis within the root occurring in the meristematic region and indicate that the penultimate step of GA biosynthesis, GA 20-oxidation, is required in both the meristem and elongation zone.

Key words gibberellin action; gibberellin metabolism; root apical meristem; root elongation zone; tissue-specific gibberellin depletion; tissue-specific mutant rescue.

This article is protected by copyright. All rights reserved

Accepted Article

Introduction

The action of the plant hormone gibberellin (GA) is necessary for normal root growth, although lower GA concentrations are required to achieve maximal rates of root elongation than for the shoot (Tanimoto, 1994; 2012). Indeed, supra-optimal GA concentrations can be inhibitory for root growth (Coelho *et al*., 2013; Inada and Shimmen, 2000). Root elongation proceeds by two mechanisms: cell replication within the root apical meristem (RAM) and cell elongation in the elongation zone (EZ). The RAM is the source of new cells within the root and plays a critical role in defining the lineages of the cell files that result from meristematic divisions. It is located at the distal tip of the root, next to a non-dividing group of cells known as the quiescent centre (QC) (Dinneny and Benfey, 2008; Nawy *et al*., 2005). As their neighbouring initial cells divide, one of the daughter cells is disconnected from the QC and then differentiates into distinct tissues. The cell files are attached and cannot move relative to one another, consequentially causing a spatial relationship that is indicative of the cell's age, with the youngest cells near the root tip getting progressively older as their distance from the QC increases (Benfey and Scheres, 2000). Tissue-specific suppression of GA signal transduction has demonstrated that this hormone determines both the size of the RAM, i.e. the number of divisions before the cells exit into the transition zone (Achard *et al*., 2009; Ubeda-Tomas *et al*., 2009) and the final cell length achieved within the EZ (Ubeda-Tomas *et al*., 2008). In both cases, GA acts in the endodermis to allow the coordinated growth of the root cell files (Ubeda-Tomas *et al*., 2009; Ubeda-Tomas *et al*., 2008).

Comparison of the growth of cultured roots of wild-type and GA-deficient tomato indicated that roots are autonomous for GA production, which is close to saturating for wild-type root growth (Butcher *et al*., 1990). It was shown from grafting experiments with *Arabidopsis thaliana* (Arabidopsis) that the root stocks could restore the growth of GA-deficient scions by supplying the GA precursor, GA_{12}, while later metabolites are not mobile (Regnault *et al*., 2015). GA_{12} is biosynthesised from the common diterpene precursor *trans*-geranylgeranyl diphosphate by the sequential action of the terpene cyclases *ent*-copalyl diphosphate synthase (CPS) and *ent*-kaurene synthase and the cytochrome P450 monooxygenases *ent*-kaurene

This article is protected by copyright. All rights reserved

oxidase and *ent*-kaurenoic acid oxidase (reviewed by Hedden and Thomas, 2012). GA_{12} is converted to the biologically active GA_4 by the 2-oxoglutarate-dependent dioxygenases (2ODDs) GA 20-oxidase (GA20ox) and GA 3-oxidase (GA3ox) (Fig. 1). These last two enzymes are encoded by small gene families, comprising five and four members, respectively, in Arabidopsis (Hedden and Phillips, 2000). Two further clades of 2ODDs deactivate GAs by 2β-hydroxylation, members of one acting primarily on C_{19}-GAs, including the biologically active forms, and of the other acting on C_{20}-GA precursors, including GA_{12}. In Arabidopsis these two GA 2-oxidase (GA2ox) clades contain five and at least two functional members, respectively (Schomburg *et al*., 2003; Thomas *et al*., 1999; Hedden and Phillips, 2000). The 2ODDs are major sites of regulation of GA content, with GA20ox activity limiting the concentration of biologically active GAs in many species, including Arabidopsis (Coles *et al*., 1999; Huang *et al*., 1998). Members of the 2ODD families show specificity in terms of regulation and tissue expression, but there is partial redundancy, with three GA20ox enzymes, GA20ox1, -2, -3 (Plackett *et al*., 2012; Rieu *et al*., 2008), and the two GA3ox paralogues GA3ox1 and -2 (Mitchum *et al*., 2006), largely responsible for bioactive GA production required for the proper development of vegetative tissues, including root growth, in Arabidopsis.

On the basis of transcript abundance, the root tip is indicated to be the main site of GA biosynthesis in the Arabidopsis root, while several *GA2ox* genes are expressed in the mature region of the root (Dugardeyn *et al*., 2008). Transcripts for a majority of GA-biosynthetic genes, including *CPS* are more abundant in the endodermis than other tissues, while *GA20ox1* mRNA accumulates in the cortex. The indication that the endodermis may be a major site of GA biosynthesis is of particular interest given that functional studies revealed that this tissue is also the site of GA action (Ubeda-Tomas *et al*., 2009; Ubeda-Tomas *et al*., 2008). Furthermore, the accumulation of fluorescence in the endodermis when GA-fluorescein probes were applied to Arabidopsis roots suggests the existence of mechanisms to concentrate GAs within this tissue (Shani *et al*., 2013). Indeed, transcript for the NPF3 transporter, which was shown to transport the GA_3 fluorescent probe as well as GA_4 and other C_{19}-GAs into *Xenopus* oocytes, accumulates to higher levels in the endodermis than in other tissues (Tal *et al*., 2015). Rizza *et al*. (2017) used a Fluorescence Resonance Energy Transfer (FRET) FRET-based, nuclear-targeted biosensor (nlsGPS1) to visualize and provide relative

This article is protected by copyright. All rights reserved

Accepted Article

quantification of nuclear GA_4 levels within the Arabidopsis root. The output from the sensor indicated a gradient of bioactive GA concentration along the primary root axis increasing with distance from the QC and peaking in the elongation zone. In contrast to the results reported by Shani *et al*. (2013), this peak of GA concentration was observed not only in the endodermis, but also in the cortical and epidermal cells.

Here we describe further approaches to define the sites of GA biosynthesis and action within the Arabidopsis root. We use tissue-specific promoters to drive expression of a C_{20}-GA2ox, *AtGA2ox7*, and a C_{19}-GA2ox, *AtGA2ox2* in the Col-0 ecotype, the first expected to act at the site of synthesis, whereas the second could act at the site of synthesis and the site of action. The same promoters are used to express functional *AtGA20ox1* in the *atga20ox1, atga20ox2, atga20ox3* triple mutant and to express *AtGA3ox1* in the *atga3ox1, atga3ox2* double mutant, both stacked mutants being extreme dwarfs with short roots (Mitchum *et al*., 2006; Plackett *et al*., 2012). The degree of rescue should indicate the location of the reactions lacking in the mutant lines. The extent to which shoot-derived GAs contribute to promotion of root growth is determined by driving expression of the same effector genes from the shoot-specific CHLOROPHYLL A/B-BINDING PROTEIN (CAB) promoter.

Materials and methods

Plant Material

Arabidopsis thaliana ecotype Col-0 was used as wild type in all experiments. The *ga20ox1 ga20ox2 ga20ox3* triple mutant (Plackett et al. 2012) and the *AtGA20ox1::GUS* (Hay et al. 2002) and *AtGA20ox2::GUS* (Frigerio et al. 2006) reporter lines are as previously published. The *ga3ox1 ga3ox2* double mutant and *AtGA3ox1::GUS* and *AtGA3ox2::GUS* lines are as described in Mitchum *et al*., (2006) and were provided by Dr Tai-ping Sun, who also provided the *ga1-3* (Col-0) mutant line containing the mutation in CPS that was originally found in *Ler* and was back-crossed to Col-0 six times (Tyler *et al*., 2004). The reporter lines are translational fusions incorporating promoter and exon and intron sequences. The *AtGA2ox6::GUS* transcriptional reporter line was provided by Dr Sharyn Perry (Wang et al. 2004).

This article is protected by copyright. All rights reserved

Accepted Article

Growth Conditions and Replication

Seeds to be grown for seed production, crossing or characterisation were surface sterilised with 10% bleach, rinsed and then imbibed in water or 50 μm GA_4 for three days at 4ºC in the dark before being sown on Levington's compost. Seeds imbibed in GA_4 were rinsed 5 times in H_2O before planting. Plants were grown in a controlled environment in 16-h days (150 $\mu mol^{-2}.sec^{-1}$) at 24/18ºC (day/night) temperatures. For measurement of root growth, after imbibition on 50 μm GA_4 and washing, seeds were grown on medium containing 0.5% Gelrite, 1% sucrose, half-strength Murashige-Skoog medium at pH of 5.8 on plates placed at an angle of 10° to the vertical in continuous light (150 $\mu mol/m^2/sec$). For measurement of root length, 2 (pseudo-replicate) or 3 plants of each line were grown on each plate so that the number of plates used was also the biological replication. Hence, there were 5 or 6 biological replicates per line for measurement of root length with 2 or 3 roots (plants) per biological replicate. For meristem and cell size measurements a single plant per plate was used and there were 5 biological replicates. Also for cell size, five (pseudo-replicate) cells were measured for each biological replicate plant. Randomized complete block designs were used with the plates being statistical blocks. For comparison of the effects of each promoter on root length, meristem size and final cortical cell length, the median lines in terms of root length for each promoter were grown together on plates, one line for each promoter per plate with 15 plates as replicates.

Activity of recombinant AtGA2ox2 fusions and AtGA2ox7

In order to produce plasmid constructs allowing expression of GA2ox2 fused to EYFP, the *EYFP* coding region was amplified by PCR and cloned into pET-32a (Novagen). Primer sequences are listed in Table S1. The *AtGA2ox2* coding region was amplified from a cDNA clone by PCR (Thomas *et al.,* 1999) and cloned into the pET-32a constructs containing *EYFP* sequences to produce the N and C-terminal expression constructs N-RB-YFP-*AtGA2ox2*:pET-32a and C-RB-*AtGA2ox2*:YFP:pET-32a. *AtGA2ox7* was amplified from *35S::GA2ox7* in pRMA1, provided by Dr R. Amasino (Schomburg et al. 2003), to introduce *Bam*HI and *Sal*I restriction sites and then ligated into pET-32a. The constructs were expressed in *E. coli* Rosetta 2 (DE3 pLysS) cells (Merck), lysates prepared and GA2ox activity determined by incubating with ^{14}C-labelled GA substrates (Prof L.N. Mander, Australian National University, Canberra ACT, Australia) as previously described (Ward *et al*., 2010). Where

This article is protected by copyright. All rights reserved

Accepted Article

necessary, product identity was confirmed by combined gas chromatography-mass spectrometry as described previously (MacMillan *et al*., 1997), except that samples were run on a MAT95XP mass spectrometer coupled to Trace GC (ThermoElectron)(Rieu *et al*., 2008) operated in full-scan mode.

Production of transgenic Arabidopsis with tissue-specific expression

The constructs for Arabidopsis transformation were produced using the Gateway cloning system. The *YFP:AtGA2ox2* fusion was inserted downstream of the tissue specific promoters within the gateway pENTR11 entry plasmid (Marques-Bueno et al. 2016) acquired from the Nottingham stock center (NASC). *AtGA2ox2* was then excised using *Bam*HI and *Sal*I and replaced with *AtGA2ox7*, *AtGA20ox1* and *AtGA3ox1*. The constructs were transferred to the pGBW7 binary vector following a standard Invitrogen LR reaction. The constructs in pGWB7 were transformed into *Agrobacterium tumefaciens* strain GV3101, and then into Arabidopsis by the floral dip method (Clough and Bent, 1998). Plants were selected on hygromycin to obtain at least 10 independent T1 lines, segregation analysis was then performed to create at least 4 stable single insertion homozygous lines for physiological analysis. Stable homozygous, single insertion, lines were taken through to the T4 generation before subsequent genotyping and phenotyping.

Plant phenotype analysis

To examine root growth, seedlings were grown on solid MS Gelrite medium for 7 d in order for the growth rates of GA deficient mutants to reach maximum (Achard *et al*., 2009). Seedlings were then mounted on slides in 10 μM propidium iodide solution to achieve counterstaining of cell walls around the cortical cells. Confocal microscopy images were acquired using a Leica TCS-SP confocal microscope (Leica, Milton Keynes, UK). EYFP was excited at 488 nm from an argon laser and the propidium iodide was visualised at 514 nm. Fluorescence emission for the EYFP was collected between 505 and 530 nm. Fluorescence images were processed using Leica LAS AF Light and Adobe Photoshop. Subsequently images were analysed using LAS AF lite, allowing meristem and cell size to be measured (Fig. S1). Measurements of cell length were taken after root hairs became visible.

This article is protected by copyright. All rights reserved

Accepted Article

Plants for assessment of shoot phenotype were grown on compost in 5.5-cm pots as described above and photographed 3 and 6 weeks after germination.

Histochemical GUS assays and microscopy

To visualize GUS expression, whole plants were placed in a substrate buffer (100 mM sodium phosphate, pH 7, 0.5 mM potassium ferrocyanide, 0.5 mM potassium ferricyanide, and 1 mM 5-bromo-4-chloro-3-indolyl glucuronide) and were incubated overnight in the dark at 37°C. Chlorophyll was cleared from stained tissue by incubating in 70 % (v/v) ethanol. Whole plants stained with GUS were observed and photographed after decolouration using an Olympus SZ-PT stereomicroscope.

For sectioning, GUS samples were fixed with 2.5% glutaraldehyde and 4% paraformaldehyde in 0.1 M sodium phosphate buffer (pH 7.2) for 2.5 h at 4°C. After this, three washes with phosphate buffer were performed. All fixed tissues were dehydrated in a graded series of ethanol, then infiltrated, first with a propylene oxide and then with propylene oxide and Spurr's resin mixture. The samples were then immersed in Spurr's resin overnight at 4°C. Finally, the samples were embedded in Spurr resin. Blocks were sectioned in semi-thin sections on a Leica EM UC6 ultramicrotome. Semi-thin sections (1 μm thick) of material prepared for GUS expression were mounted in dibutylphthalate polystyrene Xyleneand observed with a Leica DMR light microscope. The micrographs were captured using Leica QM500 image analysis software.

Statistical Analysis. Analysis of variance (ANOVA) was used to test (using the F-test) the overall statistical significance of difference between lines for the root, meristem and cell length data. The analysis took account of the design structure with plates being blocks and sections on plates being plots, with any variation due to pseudo-replicates (roots within plants, or cells within plants) being separated from the biological variation. The standard error of the difference (SED) on the residual degrees of freedom (df) from ANOVA was used to calculate the least significant difference (LSD) at the 5% ($p = 0.05$) and 1% ($p=0.01$) levels of significance. The LSDs were used to assign statistical significance to differences between the means of most relevant pairs of lines. Homogeneity of variance over the lines was checked by inspecting plots of residuals and, where required, a natural log transformation was applied

This article is protected by copyright. All rights reserved

Accepted Article

with comparisons of means being made on the transformed scale (see figure legends). The Genstat (2009, Twelfth Edition, © VSN International Ltd, Hemel Hempstead, UK) statistical package was used for this analysis.

Results

Expression of GA-metabolism reporter genes in roots

First the expression domains of GA 2ODD genes in the root were investigated using GUS reporters. For *AtGA20ox1* and *AtGA20ox2*, the reporters comprised 1.5 kbp of promoter sequence and the first two exons and introns upstream of GUS (Plackett et al. 2012). GUS staining for the *AtGA20ox1* reporter indicated expression in both the meristem and elongation zone with less expression in the transition zone (Fig 2A). Within the elongation zone, expression was confined to the cortical cells (Fig. 2B and C). GUS staining for the *AtGA20ox2* reporter was much weaker than for *AtGA20ox1*, but some staining was detected in the endodermis of the elongation zone (Fig. 2D). Although we were not able to determine its expression profile, data reported by Dugaredeyn et al. (2008) show expression of *AtGA20ox3* in roots with a similar distribution to *AtGA20ox2*. Mitchum et al. (2005) reported expression from a *AtGA3ox1:GUS* reporter within the stele throughout the root, except in the tip (meristem and elongation zone). A root cross-section in the translational fusion reporter line indicates that expression is in the pericycle, particularly at the metaxylem poles, with some staining in the adjacent endodermal cells (Fig. 2E). Mitchum et al. (2005) found a similar expression profile in roots for *AtGA3ox2*, with additional GUS expression in the elongation zone, quiescent centre and columella, but not in the meristem. In cross section through the elongation zone, expression is indicated throughout the stele and also in the endodermis (Fig. 2F).

Expression analysis by real-time quantitative RT-PCR indicates that *GA2ox6* is the most highly expressed C_{19}-*GA2ox* gene in roots (Rieu et al. 2008). We examined the expression domain of this GA-inactivation gene within the root using a *GA2ox6::GUS* transcriptional reporter line (Wang et al. 2004). Expression was present throughout the differentiated root and absent from the root tip (Fig. 2G), but in contrast to *GA3ox1*, was present in all cell types (Fig. 1H).

This article is protected by copyright. All rights reserved

Accepted Article

Defining promoters for targeted tissue and stage-specific root expression

In order to determine the relevance of the observed expression domains in the root, the sites of GA production necessary for promotion of root growth were defined by tissue-specific GA-inactivation or mutant rescue. The promoters selected to drive tissue-specific expression are listed in Table 1. A 2-kb promoter sequence from the *GLABRA2* (*GL2*) gene was used to confine expression to epidermal cells of the root. Expression occurs in cells outside a periclinal cortical cell wall and extends from the meristem to the root hair zone, with most intense expression in the differentiation zone (Masucci *et al*., 1996). The *GL2* expression domain is defined by a 500-bp fragment located between positions -840 and -1340 in the 5' region of the gene (Hung *et al*., 1998).

Co2 expression within the root is confined to the meristematic region of the cortex, its root expression domain conferred by a 500-bp promoter sequence immediately upstream of the 5' end of the open reading frame (Heidstra *et al*., 2004). Publicly available data https://www.arabidopsis.org/servlets/TairObject?type=locus&name=At1g62500 indicates expression of *Co2* also in numerous aerial organs, including juvenile rosette leaves and inflorescence, with peaks of expression within the carpel and ovary. *Co2* is highly expressed at the shoot apex during the vegetative, inflorescence and transition stages, more specifically within the rib meristem and peripheral zone of the shoot apical meristem (SAM). The Co2 promoter was first used by Mustroph *et al*. (2009) as part of a cell sorting experiment investigating plants response to hypoxia.

The *CoR* promoter was shown by fluorescence-activated cell sorting of root cells to be expressed specifically within the cortex of the elongation zone (Dinneny *et al*., 2008). Outside of the root it is expressed in germinating seeds and seedlings, leaves, reproductive organs and in the rib meristem and peripheral region of the SAM. A 500-bp sequence upstream of the start codon was used as this has been shown by green fluorescent protein (GFP) targeted expression to confirm its expression pattern in the root (Vasesva *et al*., 2018).

SCARECROW (*SCR*) encodes a GRAS transcription factor that is expressed in cortex/endodermal initials of the developing embryo and then solely in the endodermis (Di

This article is protected by copyright. All rights reserved

Accepted Article

Laurenzio *et al*., 1996). A 2-kb 5' upstream sequence of the *SCR* gene was used to drive expression, which as well as in the root, occurs in vegetative and reproductive aerial organs in the cell layer surrounding the vascular tissues (Wysocka-Diller *et al*., 2000).

We used a 2-kb promoter sequence upstream of the start codon of *SHORTROOT* (*SHR*), which is expressed in the stele (Helariutta *et al*., 2000). Its product moves from the stele into the adjacent endodermis to regulate *SCR* expression (Nakajima *et al*., 2001). It is expressed also in aerial tissues, being strongly expressed in the peripheral zone of the SAM (Yadav *et al*., 2009) and in the leaf vasculature (Dhondt *et al*., 2010).

In order to assess the contribution of shoot-derived GAs to root growth, a 1892-bp 5' upstream sequence of the *CAB* gene was used to drive expression in green tissues in the absence of significant root expression. The *CAB* gene responds to many of the developmental signals required for chloroplast development and green tissue specification (Puente *et al*., 1996). Experiments using *CAB1::GUS* fusions have shown that in WT Arabidopsis *CAB* is first expressed in the cotyledons in response to light, and after further growth the expression is confined to the photosynthetic tissue (Yadav *et al*., 2002).

Tissue-specific GA inactivation

In order to inactivate C_{19}-GAs and C_{20}-GAs by 2β-hydroxylation, Arabidopsis Col-0 was transformed with *AtGA2ox2* and *AtGA2ox7* constructs, respectively (see Fig. 1). Their cDNAs were transformed as 5' translational fusions with *YFP* in constructs containing the promoters listed in the previous section (Table S2). AtGA2ox2 has been previously shown by *in vitro* enzyme assays with bacterial expressed protein to be specific for C_{19}-GAs (Thomas *et al*., 1999). In order to confirm that YFP fusions retained enzyme activity, the activity of N- and C-fusions produced in *E. coli* was compared with that of AtGA2ox2 against [17-^{14}C]GA_9 and [17-^{14}C]GA_4 as substrates. HPLC analysis of the products demonstrated that both YFP fusion proteins were active with both substrates (Fig. S2). Therefore, it was decided to use N-terminal YFP fusions for each of the effector proteins. The assumption that the fusion proteins retained enzymatic function is supported by their expression from the CAB promoter, which produced the expected shoot phenotype (see below). The specificity of AtGA2ox7 was confirmed by incubating recombinant enzyme with ^{14}C-labelled substrates: the C_{20}-GAs,

This article is protected by copyright. All rights reserved

GA_{12} and GA_{24}, and the C_{19}-GAs, GA_9 and GA_4 (Fig. S3). While both C_{20}-GAs were 2β-hydroxylated by the enzyme, we could detect no activity against GA_9 and GA_4. GA_{12} was metabolised by AtGA2ox7 to GA_{110} (2β-hydroxyGA_{12}), and GA_{24} was converted to a product consistent with the previously undescribed 2β-hydroxyGA_{24}.

Three to six homozygous T3 lines with single inserts were selected for each transformed construct and the presence of the transgene was confirmed by PCR. The expression domains within the root were confirmed by imaging YFP fluorescence using confocal microscopy (shown for representative lines for each promoter in Fig. S4). Root lengths, as well as meristem and final cortical cell lengths (see Fig. S1) were determined in seedlings 7 days after germination and compared with those for Col-0 and the highly GA-deficient *ga1-3* mutant. The data for three representative *YFP-AtGA2ox2*-expressing lines for each construct are shown in Fig. S5, while the median lines in terms of root length for each *AtGA2ox2*-containing construct are compared in Fig. 3. With the exception of *CAB*, each promoter driving *YFP-AtGA2ox2* resulted in a reduction in root length, with *SCR* having the most severe effect and *SHR* producing a relatively small reduction. *SCR*, *Co2* and *GL2*, but not the other promoters, reduced meristem size, while *SCR* and particularly *CoR* reduced final cell length. The equivalent data for the *promoter:YFP-AtGA2ox7* lines are presented in Fig. S6 and Fig. 4. The effect of these constructs on root growth was less severe than for the *AtGA2ox2* constructs, but some reduction in root length was obtained with *SCR*, *CoR*, *Co2* and *GL2*. Significant ($p<0.01$, LSD) reductions in meristem size compared to Col-0 were found with the *SCR*, *Co2* and *GL2* promoters, while *SCR*, *CoR* and *GL2* also produced shorter cortical cells.

The effect of the ectopic gene expression on growth of the shoot was assessed at 3 and 6 weeks after sowing on compost. Results for the *AtGA2ox2* effector are shown in Fig. S7. Most severe dwarfism was obtained with the *CAB* promoter, while some lines transformed with *CoR:YFP-GA2ox2* also exhibited substantial dwarfism. Mild dwarfism was noted for plants harbouring genes driven by the other promoters, except for *SHR:YFP-GA2ox2* plants, which were identical to Col-0. In contrast to *AtGA2ox2*, expression of *AtGA2ox7* produced substantial shoot dwarfism regardless of the promoter (Fig. S8). In this case, *CAB* and *Co2*

This article is protected by copyright. All rights reserved

Accepted Article

were the most effective promoters, with *SCR* and *GL2* intermediate, and *CoR* and *SHR* producing milder dwarfism.

Rescue of the *ga20ox1, ga20ox2, ga20ox3* triple mutant

Loss of *AtGA20ox1*, *AtGA20ox2* and *AtGA20ox3*, which are three of the five *GA20ox* genes in Arabidopsis, produces a severely dwarfed, sterile plant with reduced root length and seeds which do not germinate without application of GA (Plackett et al. 2012). The triple mutant was transformed with genes in which *YFP-AtGA20ox1* was downstream of the same tissue-specific promoters described above. The root expression domains were confirmed in representative plants for each construct by confocal microscopy (Fig. S9). Total root lengths, meristem and final cortical cell lengths were determined 7 days after germination and compared with Col-0 and the triple *ga20ox* mutant. The data for three lines are presented in Fig. S10, and for the median lines for each construct, Col-0 and triple *ga20ox* mutant in Fig. 5. Complete rescue of root growth, including meristem size and cortical cell length, was obtained with the *SCR* promoter, while *Co2*, *GL2* and *CAB* provided partial rescue of root length. In the case of *Co2* and *GL2*, both meristem and cell lengths were promoted, while the *CAB* promoter increased only cell length. No rescue was obtained with the *SHR* or *CoR* promoter. The failure of *CoR:YFP-AtGA20ox1* to rescue cell length, whereas there was slight rescue by the *Co2* promoter, suggested that cell elongation required GA 20-oxidation in the meristem. Indeed, full rescue of cell elongation and root growth was obtained by combining *CoR:YFP-AtGA20ox1* with *Co2:YFP-AtGA20ox1* in the *ga20ox* triple mutant (Fig. 6).

The effect of the transgenes on growth of the shoots is illustrated in Fig. S11, in which the lines are compared with Col-0 and GA-deficient triple *ga20ox* and *ga1-3* mutants. Growth of plants expressing *CAB:YFP-GA20ox1* was slightly greater than for the WT, and the *SCR* and *Co2* promoters gave almost full mutant rescue. Expression from the *GL2* promoter also gave substantial rescue, but the *CoR* and *SHR* promoters driving *YFP-GA20ox1* produced no growth stimulation in the triple *ga20ox* mutant.

Rescue of the *ga3ox1 ga3ox2* double mutant

The same tissue-specific promoters were used to drive expression of *YFP:AtGA3ox1* in the *ga3ox1 ga3ox2* double mutant; the spatial distribution of YFP in roots of the transgenic lines

This article is protected by copyright. All rights reserved

Accepted Article

was determined by confocal microscopy (Fig. S12). Apart from in their expected root expression domains, the GL2 and CAB promoters also produced fluorescence in the columella. Total root lengths, meristem and final cortical cell lengths for three lines are shown in Fig. S13, and the median plants for each construct are compared with Col-0 and the double *ga3ox* mutant in Fig. 7. All promoters driving *YFP:AtGA3ox1* rescued root length to some extent, with roots in the *SHR*, *SCR*, *CoR* and *GL2* promoter lines not being significantly ($p>0.05$, LSD) shorter than the Col-0 wild type. In the *Co2* and *CAB* lines there was partial rescue of root length. Meristem length in the *SHR*, *SCR* and *Co2* lines was not significantly different ($p>0.05$, LSD) from that in Col-0, while there was partial rescue of meristem size in the *CoR* and *GL2* lines, but none in the *CAB* lines. There was substantial rescue of final cortical cell length with all promoters, with only the *Co2* line producing cells significantly ($p<0.05$, LSD) shorter than those in Col-0.

Similar to what was observed for root growth, the constructs fully restored growth of the shoots, regardless of which promoter was used (Fig. S14).

Discussion

Rizza et al. (2017), using a nuclear targeted biosensor nlsGPS1, reported a gradient of bioactive GA from the root tip to the elongation zone that was exaggerated when GA_4 was applied to the root. This indicates the existence of a transport system that concentrates bioactive GAs in this zone. The results of Shani et al (2013) from application of fluorescein-conjugated GA_4 and GA_3 probes to the Arabidopsis root support this conclusion, although, while Shani et al. (2013) found accumulation of the probe within the endodermis, the results of Rizza et al. (2017) suggest wider distribution of GA within the elongation zone. However, these findings are not in agreement with the model proposed by Band et al. (2012), which predicts that GA concentration is diluted as cells expand, as a potential mechanism to explain growth cessation. Furthermore, it has remained unclear as to whether bioactive GAs are synthesized *in situ* or are translocated to the sites of action from other tissues as final products or as precursors. The existence of a concentrating mechanism within the root, as suggested by Rizza et al. (2017) and Shani et al (2013), is compatible with movement to the elongation

This article is protected by copyright. All rights reserved

Accepted Article

zone from another site. In the present study to investigate the sites of GA biosynthesis in the root, the promoters chosen to provide cell-specific GA inactivation or mutant rescue were based on their established expression domains within the root, which were confirmed by expressing YFP fusions. This multipronged approach should enhance the robustness of the results, which could be influenced by differences in the expression levels of the ectopic genes compared with those of the native GA-biosynthesis genes.

The selected promoters are also active in aerial tissues and several of the constructs modified shoot as well as root growth. In order to determine the extent to which root growth is influenced by the shoot, the same effector open reading frames (ORFs) were expressed from the shoot-specific *CAB* promoter. While expression of the GA-inactivation *AtGA2ox2* and *AtGA2ox7* cDNAs from *CAB* resulted in severe dwarfing of the shoot, these constructs had no effect on root growth, confirming that roots can be autonomous for GA production. It has been reported that application of the GA-biosynthesis inhibitor uniconazole to shoots of Arabidopsis seedlings stimulates root elongation and up-regulates the feedback-regulated *GA20ox* and *GA3ox* genes in roots (Bidadi et al. 2009). Bidadi et al (2009) argued that, under standard conditions, root growth is promoted partially by GA or a precursor transported from the shoot, but that, in the absence of this source of promotion, the plant can enhance *in situ* GA production to (more than) compensate. Grafting experiments have shown that the shoot can provide the GA precursor GA_{12} to rescue root growth in GA mutants with lesions early in the GA-biosynthetic pathway, while later intermediates and the active hormone are apparently not transported (Regnault et al. 2015). Transformation of the *ga20ox* triple mutant with *CAB::YFP:AtGA20ox1* and of the *ga3ox* double mutant with *CAB::YFP:AtGA3ox1* gave partial recovery of root length and cell length, but not meristem size, indicating that shoot-derived C_{19}-GAs can make a small contribution to root growth, even if GA_{12} is the main form transported from the shoots.

Gibberellin signalling is required for normal cell production in the meristem (Achard et al. 2009; Ubeda-Tomas et al. 2009) and for cell elongation (Ubeda-Tomas et al. 2008), with the endodermis identified as the major site of GA action. Our results based on rescue of the triple *ga20ox* mutant indicate that GA 20-oxidation in the endodermis (SCR promoter), cortex (Co2) or epidermis (GL2) is sufficient to stimulate root growth, with the endodermal activity

This article is protected by copyright. All rights reserved

Accepted Article

having the largest influence (Fig. 5). On the basis of meta-analysis of gene expression data, Dugardeyn et al. (2008) concluded that many of the genes that influence GA production in the Arabidopsis root are most highly expressed in the endodermis, but also have expression in the cortex. Expression of *AtGA2ox2* and *AtGA2ox7* from the *Co2* promoter, which is active in cortical cells of the meristem, reduced meristem size, but not cell length, while expression of these effectors from *CoR*, which promotes expression in the cortex of the EZ, reduced cell length, but not meristem size. This is consistent with GA being required in both the meristem and EZ for normal root growth. It also suggests that the cortex is an important site of GA biosynthesis. However, while *AtGA20ox1* expression from Co2 gave partial rescue of both meristem and cell size in the triple *ga20ox* mutant, expression of *AtGA20ox1* from *CoR* gave no rescue, even of cortical cell length. On the basis of GUS staining in lines expressing the *AtGA20ox1* reporter, the endogenous gene is expressed specifically in cortical cells of the EZ as well as in the meristem (Fig. 2A-C). The unexpected lack of rescue by *CoR::YFP:AtGA20ox1* may indicate insufficient availability of its C_{20}-GA substrates in the EZ, which may be provided by the meristem . This was tested by crossing *CoR::YFP:AtGA20ox1* with *Co2::YFP:AtGA20ox1* to restore GA20ox activity in the cortex of the meristem and EZ. Full rescue of the root phenotype in the cross confirmed that GA biosynthesis, and potentially activity, within the meristem is necessary for cell elongation. If the meristem provides C_{20}-GA substrate for GA 20-oxidation in the EZ cortex, this would not be GA_{12}, which would be depleted by GA20ox activity, when in fact *Co2::YFP:AtGA20ox1* restored some cell elongation, although this could also be explained by provision of active GA to the EZ. Full rescue of cell elongation was obtained with *CoR::YFP:AtGA3ox1* in the *ga3ox1*/ga3ox2 background, indicating the presence of its substrate GA_9 in the cortex and that its product GA_4 is able to move to the site of action in the endodermis. It is also possible that GA action in the cortex enables some cell expansion. This rescue of cell elongation by *CoR::YFP:AtGA3ox1* indicates that GA biosynthesis and/or action in the meristem is not required for cell elongation, although *CoR::YFP:AtGA3ox1* also provided partial rescue of meristem size suggesting movement of GA_4 from the EZ to the meristem. It is necessary to consider the up-regulation of *GA20ox* genes in the GA deficient mutants due to feedback regulation (Phillips et al. 1995) that could increase GA_9 production and availability in cells where it is normally limiting.

This article is protected by copyright. All rights reserved

Accepted Article

On the basis of reporter gene expression, Mitchum et al. (2006) showed that *AtGA3ox1* is expressed in the mature, non-elongating region of the root and our results with the same reporter lines indicate that this expression is in the pericycle cells of the stele. Using an equivalent reporter gene, Bidadi et al. (2009) obtained GUS staining in the EZ and root tip after shoot-applied uniconazole. This indicates that the gene is expressed in these regions, albeit normally at very low levels. *AtGA3ox2* is also expressed in the mature root, but in addition is expressed in the EZ, quiescent centre and columella, but apparently not in the meristem (Mitchum et al. 2006). Taken with the nlsGPS1 reporter data, this could indicate that small quantities of GA are activated around the QC providing a low concentration of GA required for cell division. Then, as the cells reach the transition zone, the higher expression of *GA3ox1* increases the amount of bioactive GA to promote cell elongation. We show that within the EZ, *AtGA3ox2* is expressed in the stele and endodermis, with some expression in cortical cells. This expression domain is consistent with the complete rescue of root growth in *ga3ox1 ga3ox2* by expression of *AtGA3ox1*, which encodes a functionally identical enzyme to AtGA3ox2, from the *SHR* (stele), *SCR* (endodermis) and *CoR* (cortex) promoters. Expression in the epidermis from the *GL2* promoter also gave strong rescue of root growth, although there is no indication that *GA3ox* genes are normally expressed in this cell file. This rescue demonstrates that these tissues have access to the GA3ox substrate GA_9 and that the product GA_4 is accessible to the site of action in the endodermis. The absence of *AtGA3ox1* causes a small reduction in root growth, whereas loss of AtGA3ox2 has no effect (Mitchum et al. 2006). This would suggest that GA_4 produced from GA_9 in the stele makes a contribution to promotion of root growth. While there is evidence for the long-distance movement of GA_{12}, but not of GA_9, from the shoot to roots (Regnault et al. 2015), there may be some limited transport of of GA_9 from the shoot or it may be produced in the phloem. However, *SHR::YFP:AtGA20ox1* failed completely to rescue root growth in the triple *ga20ox* mutant, indicating that the *SHR* expression domain does not overlap with those of *AtGA20ox1, AtGA20ox2* or *AtGA20ox3*.

Full rescue of the growth of aerial organs in the *ga3ox1 ga3ox2* mutant was obtained with all promoters driving *AtGA3ox1* expression, while no rescue of the triple *ga20ox* mutant occurred when *AtGA20ox1* was expressed from *SHR* or *CoR.* The other promoters gave different degrees of triple *ga20ox* rescue, with *CAB* and *SCR* proving the most effective. It would

This article is protected by copyright. All rights reserved

Accepted Article

appear that the cells expressing *SHR* and *CoR* have limited access to GA_{12} or other C_{20}-GA intermediates, whereas GA_9 is freely available in all the expression domains tested. It is also possible that GA_9 is not released from these cells or, less likely, that there is cell-specific instability of GA20ox1. Expression of the C_{20}-GA-inactivation cDNA *AtGA2ox7* was generally more effective than that of the *C_{19}-GA2ox*, *AtGA2ox2* at reducing shoot growth with almost all promoters, except for *CAB*, which gave strong dwarfism with both effector genes. This may reflect the strength and broad expression domain of the *CAB* promoter in shoots. For *AtGA2ox7* expression, the *SHR* and *CoR* promoters were the least effective, consistent with the *GA20ox* mutant rescue and reinforcing the conclusion that the stele and cortex of the EZ have least access to C_{20}-GAs. In contrast, with the exception of *CAB*, the *CoR* promoter driving *YFP:AtGA2ox2* was the most dwarfing, with *SCR* having some effect. If there is high mobility between tissues of GA_9 and GA_4, as suggested by the *ga3ox* mutant rescue, then, providing their formation occurs in more than one tissue type, inactivation restricted to specific tissues will be ineffective. The dwarfing obtained with *CoR* and *SCR* promoters could reflect the fact that they are active at, or close to, the site of GA action.

In conclusion, the results, which are summarized in Fig. 8, support previous indications that roots and shoots are autonomous for GA production and that GA is required for cell division in the root meristem and elongation in the EZ. The cortex and endodermis are important sites of GA biosynthesis, but GA biosynthesis (GA20ox activity) and/or cell elongation in the cortex of the EZ are dependent on GA production and/or action in the meristem. The meristem may also supply GA and precursors to the EZ. While transport of C_{20}-GAs or earlier precursors of GA biosynthesis between root tissues is restricted, the rescue of root growth by *AtGA3ox1* in the *ga3ox* double mutant indicates efficient movement of C_{19}-GAs between tissues. Partial restoration of cell elongation, but not cell division, by shoot expression of *GA20ox1* or *GA3ox1* in the respective mutants indicate some movement of C_{19}-GAs from shoot to root, despite GA_{12} being the major transport form (Regnault et a. (2015).

Acknowledgements: We are grateful to Dr Tai-ping Sun, Duke University, for the *ga3ox1 ga3ox2* and *ga1-3*(Col-0) mutants, to Dr Sharyn Perry, University of Kentucky, for the AtGA2ox6::GUS reporter line, to Dr Susana Ubeda-Tomas, University of Nottingham, for the

This article is protected by copyright. All rights reserved

Accepted Article

pENTR11:SCR:GID1:YFP plasmid, to Dr Richard Amasino, University of Wisconsin, for the 35S:AtGA2ox7 plasmid and to I. Pearman, A. Griffin and other glasshouse staff at Rothamsted Research for plant husbandry. This work was supported by a Lawes Agricultural Trust Studentship to RB and by grant P16508, funded by the Biotechnology and Biological Sciences Research Council of the UK, which also provides support to Rothamsted Research through funding of the 20:20Wheat© (BBS/E/C/00005202) and Designing Future Wheat Integrated Strategic Programmes (BBS/E/C/000I0220; ALP and ST). PH acknowledges funding from The Czech Science Foundation (grant Nos 18-10349S and 20-17984S) and the European Regional Developmental Fund Project "Centre for Experimental Plant Biology" No. CZ.02.1.01/0.0/0.0/16_019/0000738.

Author contributions: RB, MJB, ALP, SGT and PH planned and designed the research, RB and MNFG performed the experiments, SV, MJB, ALP, SGT and PH supervised the research, SJP carried out the statistical analysis. RB and PH wrote the manuscript, which was edited by SJP, MJB, ALP and SGT.

References

Achard P, Gusti A, Cheminant S, Alioua M, Dhondt S, Coppens F, Beemster GTS, Genschik P. 2009. Gibberellin signaling controls cell proliferation rate in Arabidopsis. *Current Biology* **19**: 1188-1193.

Benfey PN, Scheres B. 2000. Primer - Root development. *Current Biology* **10**: R813-R815.

Bidadi H, Yamaguchi S, Asahina M, Satoh S. 2009. Effects of shoot-applied gibberellin/gibberellin-biosynthesis inhibitors on root growth and expression of gibberellin biosynthesis genes in *Arabidopsis thaliana*. *Plant Root* **4**: 4-11.

Butcher DN, Clark JA, Lenton JR. 1990. Gibberellins and the growth of excised tomato roots - comparison of gib-1 mutant and wild-type and responses to applied GA_3 and 2S ,3S paclobutrazol. *Journal of Experimental Botany* **41**: 715-722.

Clough SJ, Bent AF. 1998. Floral dip: a simplified method for Agrobacterium-mediated transformation of Arabidopsis thaliana. *The Plant Journal* **16**: 735-743.

Coelho M, Colebrook EH, Lloyd DPA, Webster CP, Mooney SJ, Phillips AL, Hedden P, Whalley WR. 2013. The involvement of gibberellin signalling in the effect of soil resistance to root penetration on leaf elongation and tiller number in wheat. *Plant & Soil* **371**: 81-94.

This article is protected by copyright. All rights reserved

Accepted Article

Coles JP, Phillips AL, Croker SJ, Garcia Lepe R, Lewis MJ, Hedden P. 1999. Modification of gibberellin production and plant development in Arabidopsis by sense and antisense expression of gibberellin 20-oxidase genes. *The Plant Journal* **17**: 547-556.

Dhondt S, Coppens F, De Winter F, Swarup K, Merks RMH, Inze D, Bennett MJ, Beemster GTS. 2010. SHORT-ROOT and SCARECROW regulate leaf growth in Arabidopsis by stimulating S-phase progression of the cell cycle. *Plant Physiology* **154**: 1183-1195.

Di Laurenzio L, WysockaDiller J, Malamy JE, Pysh L, Helariutta Y, Freshour G, Hahn MG, Feldmann KA, Benfey PN. 1996. The SCARECROW gene regulates an asymmetric cell division that is essential for generating the radial organization of the Arabidopsis root. *Cell* **86**: 423-433.

Dinneny JR, Benfey PN. 2008. Plant stem cell niches: Standing the test of time. *Cell* **132**: 553-557.

Dinneny JR, Long TA, Wang JY, Jung JW, Mace D, Pointer S, Barron C, Brady SM, Schiefelbein J, Benfey PN. 2008. Cell identity mediates the response of Arabidopsis roots to abiotic stress. *Science* **320**: 942-945.

Dugardeyn J, Vandenbussche F, Van Der Straeten D. 2008. To grow or not to grow: what can we learn on ethylene-gibberellin cross-talk by in silico gene expression analysis? *Journal of Experimental Botany* **59**: 1-16.

Frigerio M, Alabadi D, Perez-Gomez J, Garcia-Carcel L, Phillips AL, Hedden P, Blazquez MA. 2006. Transcriptional regulation of gibberellin metabolism genes by auxin signaling in Arabidopsis. *Plant Physiology* **142**: 553-563.

Hay A, Kaur H, Phillips A, Hedden P, Hake S, Tsiantis M. 2002. The gibberellin pathway mediates KNOTTED1-type homeobox function in plants with different body plans. *Current Biology* **12**: 1557-1565.

Hedden P, Phillips AL. 2000. Gibberellin metabolism: new insights revealed by the genes. *Trends in Plant Science* **5**: 523-530.

Hedden P, Thomas SG. 2012. Gibberellin biosynthesis and its regulation. *Biochemical Journal* **444**: 11-25.

Heidstra R, Welch D, Scheres B. 2004. Mosaic analyses using marked activation and deletion clones dissect Arabidopsis SCARECROW action in asymmetric cell division. *Genes & Development* **18**: 1964-1969.

This article is protected by copyright. All rights reserved

Accepted Article

Helariutta Y, Fukaki H, Wysocka-Diller J, Nakajima K, Jung J, Sena G, Hauser MT, Benfey PN. 2000. The SHORT-ROOT gene controls radial patterning of the Arabidopsis root through radial signaling. *Cell* **101**: 555-567.

Huang SS, Raman AS, Ream JE, Fujiwara H, Cerny RE, Brown SM. 1998. Overexpression of 20-oxidase confers a gibberellin-overproduction phenotype in Arabidopsis. *Plant Physiology* **118**: 773-781.

Hung CY, Lin Y, Zhang M, Pollock S, Marks MD, Schiefelbein J. 1998. A common position-dependent mechanism controls cell-type patterning and GLABRA2 regulation in the root and hypocotyl epidermis of Arabidopsis. *Plant Physiology* **117**: 73-84.

Inada S, Shimmen T. 2000. Regulation of elongation growth by gibberellin in root segments of *Lemna minor*. *Plant & Cell Physiology* **41**: 932-939.

MacMillan J, Ward DA, Phillips AL, Sanchez Beltran MJ, Gaskin P, Lange T, Hedden P. 1997. Gibberellin biosynthesis from gibberellin A_{12}-aldehyde in endosperm and embryos of *Marah macrocarpus*. *Plant Physiology* **113**: 1369-1377.

Marques-Bueno MM, Morao AK, Cayrel A, Platre MP, Barberon M, Caillieux E, Colot V, Jaillais Y, Roudier F, Vert G. 2016. A versatile Multisite Gateway-compatible promoter and transgenic line collection for cell type-specific functional genomics in Arabidopsis. *The Plant Journal* **85**: 320-333.

Masucci JD, Rerie WG, Foreman DR, Zhang M, Galway ME, Marks MD, Schiefelbein JW. 1996. The homeobox gene *GLABRA2* is required for position-dependent cell differentiation in the root epidermis of *Arabidopsis thaliana*. *Development* **122**: 1253-1260.

Mitchum MG, Yamaguchi S, Hanada A, Kuwahara A, Yoshioka Y, Kato T, Tabata S, Kamiya Y, Sun TP. 2006. Distinct and overlapping roles of two gibberellin 3-oxidases in Arabidopsis development. *The Plant Journal* **45**: 804-818.

Mustroph A, Zanetti MW, Jang CJH, Holtan HE, Repetti PP, Galbraith DW, Girke T and Bailey-Serres J. 2009. Profiling translatomes of discrete cell populations resolves altered cellular priorities during hypoxia in *Arabidopsis*. *Proceedings of the National Academy of Sciences of the United States of America* **106**: 18843-18848.

Nakajima K, Sena G, Nawy T, Benfey PN. 2001. Intercellular movement of the putative transcription factor SHR in root patterning. *Nature* **413**: 307-311.

This article is protected by copyright. All rights reserved

Accepted Article

Nawy T, Lee JY, Colinas J, Wang JY, Thongrod SC, Malamy JE, Birnbaum K, Benfey PN. 2005. Transcriptional profile of the Arabidopsis root quiescent center. *The Plant Cell* **17**: 1908-1925.

Phillips AL, Ward DA, Uknes S, Appleford NEJ, Lange T, Huttly A, Gaskin P, Graebe JE, Hedden, P. 1995. Isolation and expression of three gibberellin 20-oxidase cDNA clones from *Arabidopsis. Plant Physiology* **108**: 1049-1057.

Plackett ARG, Powers SJ, Fernandez-Garcia N, Urbanova T, Takebayashi Y, Seo M, Jikumaru Y, Benlloch R, Nilsson O, Ruiz-Rivero O *et al.* 2012. Analysis of the developmental roles of the Arabidopsis gibberellin 20-oxidases demonstrates that GA20ox1, -2, and -3 are the dominant paralogs. *The Plant Cell* **24**: 941-960.

Puente P, Wei N, Deng XW. 1996. Combinatorial interplay of promoter elements constitutes the minimal determinants for light and developmental control of gene expression in Arabidopsis. *EMBO Journal* **15**: 3732-3743.

Regnault T, Daviere JM, Wild M, Sakvarelidze-Achard L, Heintz D, Bergua EC, Diaz IL, Gong F, Hedden P, Achard P. 2015. The gibberellin precursor GA_{12} acts as a long-distance growth signal in Arabidopsis. *Nature Plants* **1**: 15073.

Rieu I, Ruiz-Rivero O, Fernandez-Garcia N, Griffiths J, Powers SJ, Gong F, Linhartova T, Eriksson S, Nilsson O, Thomas SG *et al.* 2008. The gibberellin biosynthetic genes *AtGA20ox*1 and *AtGA20ox2* act, partially redundantly, to promote growth and development throughout the Arabidopsis life cycle. *The Plant Journal* **53**: 488-504.

Rizza A, Walia A, Lanquar V, Frommer W, Jones A. 2017. In vivo gibberellin gradients visualized in rapidly elongating tissues. **Nature Plants 3**: 803-813

Schomburg FM, Bizzell CM, Lee DJ, Zeevaart JAD, Amasino RM. 2003. Overexpression of a novel class of gibberellin 2-oxidases decreases gibberellin levels and creates dwarf plants. *The Plant Cell* **15**: 151-163.

Shani E, Weinstain R, Zhang Y, Castillejo C, Kaiserli E, Chory J, Tsien RY, Estelle M. 2013. Gibberellins accumulate in the elongating endodermal cells of Arabidopsis root. *Proceedings of the National Academy of Sciences of the United States of America* **110**: 4834-4839.

Tanimoto E. 1994. Interaction of gibberellin A_3 and ancymidol in the growth and cell-wall extensibility of dwarf pea roots. *Plant & Cell Physiology* **35**: 1019-1028.

This article is protected by copyright. All rights reserved

Accepted Article

Tanimoto E. 2012. Tall or short? Slender or thick? A plant strategy for regulating elongation growth of roots by low concentrations of gibberellin. *Annals of Botany* **110**: 373-381.

Tal I, Zhang Y, Jørgensen ME, Pisanty O, Barbosa ICR, Zourelidou M, Regnault T, Crocoll C, Olsen CE, Weinstain R *et al.* 2015. The *Arabidopsis* NPF3 protein is a GA transporter. *Nature Communications* **7**: 11486.

Thomas SG, Phillips AL, Hedden P. 1999. Molecular cloning and functional expression of gibberellin 2-oxidases, multifunctional enzymes involved in gibberellin deactivation. *Proceedings of the National Academy of Sciences of the United States of America* **96**: 4698-4703.

Tyler L, Thomas SG, Hu JH, Dill A, Alonso JM, Ecker JR, Sun TP. 2004. DELLA proteins and gibberellin-regulated seed germination and floral development in Arabidopsis. *Plant Physiology* **135**: 1008-1019.

Ubeda-Tomas S, Federici F, Casimiro I, Beemster GTS, Bhalerao R, Swarup R, Doerner P, Haseloff J, Bennett MJ. 2009. Gibberellin signaling in the endodermis controls Arabidopsis root meristem size. *Current Biology* **19**: 1194-1199.

Ubeda-Tomas S, Swarup R, Coates J, Swarup K, Laplaze L, Beemster GTS, Hedden P, Bhalerao R, Bennett MJ. 2008. Root growth in Arabidopsis requires gibberellin/DELLA signalling in the endodermis. *Nature Cell Biology* **10**: 625-628.

Vaseva II, Qudeimat E, Potuschak T, Du Y, Genschik P, Vandenbussche F, van der Straeten D. 2018. The plant hormone ethylene restricts *Arabidopsis* growth via the epidermis. *Proceedings of the National Academy of Sciences of the United States of America* **115**: E4130-E4139.

Wang H, Caruso LV, Downie AB, Perry SE. 2004. The embryo MADS domain protein AGAMOUS-Like 15 directly regulates expression of a gene encoding an enzyme involved in gibberellin metabolism. *The Plant Cell* **16**: 1206-1219.

Ward DA, MacMillan J, Gong F, Phillips AL, Hedden P. 2010. Gibberellin 3-oxidases in developing embryos of the southern wild cucumber, *Marah macrocarpus*. *Phytochemistry* **71**: 2010-2018.

Wysocka-Diller JW, Helariutta Y, Fukaki H, Malamy JE, Benfey PN. 2000. Molecular analysis of SCARECROW function reveals a radial patterning mechanism common to root and shoot. *Development* **127**: 595-603.

This article is protected by copyright. All rights reserved

Accepted Article

Yadav RK, Girke T, Pasala S, Xie MT, Reddy V. 2009. Gene expression map of the Arabidopsis shoot apical meristem stem cell niche. *Proceedings of the National Academy of Sciences of the United States of America* **106**: 4941-4946.

Yadav V, Kundu S, Chattopadhyay D, Negi P, Wei N, Deng XW, Chattopadhyay S. 2002. Light regulated modulation of Z-box containing promoters by photoreceptors and downstream regulatory components, COP1 and HY5, in Arabidopsis. *The Plant Journal* **31**: 741-753.

Figure Legends

Fig. 1. Biosynthetic pathway from GA_{12} to GA_4 and 2β-hydroxy catabolites, indicating the reactions catalysed by AtGA20ox1, AtGA3ox1, AtGA2ox2 and AtGA2ox7.

Fig. 2. Reporter gene (GUS) expression in roots of 7 day-old seedlings of *Arabidopsis thaliana*. (**A-C**) p*AtGA20ox1*, (**D**) p*AtGA20ox2*, (**E**) p*AtGA3ox1*, (**F**) p*AtGA3ox2,* (**G-H**) p*AtGA2ox6*. With the exception of p*AtGA2ox6:GUS*, the reporter constructs consisted of translational fusions including the final intron.

Fig. 3. Comparison of the primary root parameters for median Col-0 lines expressing *YFP-AtGA2ox2* with those of Col-0 and *ga1-3*(Col-0) in 7 day-old seedlings of *Arabidopsis thaliana*. (**A**) Primary root length. (**B**) Proximal meristem length. (**C**) Final cortical cell length. † indicates that the transgenic lines are statistically significantly different from *ga1-3* and * indicates that they are statistically significantly different from Col-0. 12 plants for each line were measured for root length with 2 plants (roots) per biological replicate (n=6), 5 plants for each line were measured for meristem and cell size (n=5), with 5 cells per biological replicate being measured. *=p<0.05, **=p<0.01, †=p<0.05 and ††=p<0.01 according to least significant difference (LSD) values (see Supporting Information Notes S1 for means, LSDs and df). Error bars indicate standard error.

Fig. 4. Comparison of the primary root parameters for median lines expressing each *YFP-AtGA2ox7* construct with Col-0 and *ga1-3* in 7 day-old seedlings of *Arabidopsis thaliana*. (**A**) Primary root length. (**B**) Proximal meristem length. (**C**) Final cortical cell length. † indicates

This article is protected by copyright. All rights reserved

Accepted Article

that the transgenic lines are statistically significantly different from *ga1-3* and * indicates that they are statistically significantly different from Col-0. 12 plants for each line were measured for root length with 2 plants (roots) per biological replicate (n=6), 5 plants for each line were measured for meristem and cell size (n=5), with 5 cells per biological replicate being measured. *=p<0.05, **=p<0.01, †=p<0.05 and ††=p<0.01 according to least significant difference (LSD) values (see Supporting Information Notes S1 for means, LSDs and df). Error bars indicate standard error.

Fig. 5. Comparison of the primary root parameters in 7 day-old seedlings of *Arabidopsis thaliana* for median lines expressing each *YFP-AtGA20ox1* construct in the *ga20ox1,2,3* triple mutant compared with those of Col-0 and the triple *ga20ox* mutant. (**A**) Primary root length. (**B**) Proximal meristem length. (**C**) Final cortical cell length. Seedlings were grown on vertical plates and lengths calculated using ImageJ. † indicates that the transgenic lines are significantly different from and *atga20ox1,2,3* and * indicates that they are significantly different from Col-0. 12 plants for each line were measured for root length with 2 plants (roots) per biological replicate (n=6), 5 plants for each line were measured for meristem and cell size (n=5), with 5 cells per biological replicate being measured. *=p<0.05, **=p<0.01, †=p<0.05 and ††=p<0.01 according to least significant difference (LSD) values (see Supporting Information Notes S1 for means, LSDs and df). Error bars indicate standard error.

Fig. 6. Combining cortical *GA20ox* expression in the meristem and elongation zone of 7 day-old seedlings of *Arabidopsis thaliana*. (**A**) YFP fluorescence in roots of a cross between *Co2:YFP-AtGA20ox1* and *CoR:YFP-AtGA20ox2* and in the parent lines. (**B**) Comparison of the lengths of the primary root, proximal meristem and final cortical cells in the cross and parent lines compared with those in Col-0 and the triple *atga20ox1,2,3* mutant. Seedlings were grown on vertical plates and lengths calculated using ImageJ. † indicates that the transgenic lines are significantly different from *ga1-3* and * indicates that they are significantly different from Col-0. 12 plants for each line were measured for root length with 2 plants (roots) per biological replicate (n=6), 5 plants for each line were measured for meristem and cell size (n=5), with 5 cells per biological replicate being measured. *=p<0.05, **=p<0.01 and ††=p<0.01 according to least significant difference (LSD) values (see Supporting Information Notes S1 for means, LSDs and df). Error bars indicate standard error.

This article is protected by copyright. All rights reserved

Accepted Article

Fig. 7. Comparison of the primary root parameters in 7 day-old seedlings of *Arabidopsis thaliana* for median lines expressing each *YFP-AtGA3ox1* construct in the *ga3ox1,2* double mutant compared with those of Col-0 and the double *ga3ox* mutant. (**A**) Primary root length. (**B**) Proximal meristem length. (**C**) Final cortical cell length. † indicates that the transgenic lines are statistically significantly different from the double *ga3ox* mutant and * indicates that they are statistically significantly different from Col-0. 12 plants for each line were measured for root length with 2 plants (roots) per biological replicate (n=6), 5 plants for each line were measured for meristem and cell size (n=5), with 5 cells per biological replicate being measured. *=$p<0.05$, **=$p<0.01$ and ††=$p<0.01$ according to least significant difference (LSD) values (see Supporting Information Notes S1 for means, LSDs and df). Error bars indicate standard error.

Fig. 8. Summary of the results showing the root domains in which expression of *AtGA2ox2* or *AtGA2ox7* produced strong (red), partial (yellow) or no inhibition of root growth (blue), or in which expression of *AtGA20ox1* or *AtGA3ox1* produced complete (red), partial (yellow) or no rescue of root growth in the *ga20ox* triple or *ga3ox* double mutants, respectively.

This article is protected by copyright. All rights reserved

Accepted Article

Table 1: Genes for which expression is targeted to specific tissues within the Arabidopsis root.

Tissue targeted	Gene with tissue specific expression	ATG code	Reference
Epidermis	GL2 – GLABRA2	At1g79840	(Masucci et al. 1996)
Cortex – Meristematic region	Co2 – Unknown protein	At1g62500	(Heidstra et al. 2004)
Cortex – Elongation zone	CoR – Unknown protein	At1g09750	(Dinneny et al. 2008)
Endodermis	SCR - SCARECROW	At3g54220	(Di Laurenzio et al. 1996)
Stele	SHR – SHORTROOT	At4g37650	(Helariutta et al. 2000)
Green tissue/shoots	CAB – Chlorophyll a/b binding protein	At1g29920	(Puente et al. 1996)

This article is protected by copyright. All rights reserved

Supporting Information

Fig. S1 The root tip indicating the regions measured.

Fig. S2 HPLC-radiochromatograms from incubations of [17-^{14}C]GA_9 and -GA_4 with cell lysates from *E. coli* transformed with *AtGA2ox2* and *YFP* fusions.

Fig. S3 HPLC-radiochromatograms from incubations of cell lysates from *E. coli* transformed with *AtGA2ox7* and ^{14}C-labelled C_{19}-GAs, GA_9 and GA_4, and C_{20}-GAs, GA_{12} and GA_{24}.

Fig. S4 YFP fluorescence in roots of representative lines expressing *YFP-AtGA2ox2* or *YFP-AtGA2ox7* in Col-0, indicating expression domains.

Fig. S5 Comparison of the primary root parameters for three lines expressing *YFP-AtGA2ox2* from tissue-specific promoters in Col-0 with those of Col-0 and *ga1-3* in 7 day-old seedlings.

Fig. S6. Comparison of the primary root parameters for three lines expressing *YFP-AtGA2ox7* from tissue-specific promoters in Col-0 with those of Col-0 and *ga1-3* in 7 day-old seedlings.

Fig. S7. The effect on shoot growth in Col-0 of expressing *AtGA2ox2* from tissue-specific promoters. 4-6 independent transformants are shown for each construct with Col-0 and *ga1-3*.

Fig. S8 The effect on shoot growth in Col-0 of expressing *AtGA2ox7* from tissue-specific promoters. 4-6 independent transformants are shown for each construct with Col-0 and ga1-3.

Fig. S9 YFP fluorescence in roots of representative lines expressing *YFP-AtGA20ox1* in the *ga20ox1,2,3* triple mutant, indicating expression domains.

Fig. S10 Comparison of the primary root parameters for three lines expressing *YFP-AtGA20ox1* from tissue-specific promoters in the *ga20ox1 ga20ox2 ga20ox3* triple mutant with those of Col-0 and the triple *ga20ox* mutant in 7 day-old seedlings.

Fig. S11 The degree of shoot growth rescue of the *ga20ox1 ga20ox2 ga20ox3* triple mutant from expressing *AtGA20ox1* from tissue-specific promoters.

Fig. S12 YFP fluorescence in roots of representative lines expressing *YFP-AtGA3ox1* in the *ga3ox1,2* double mutant, indicating expression domains.

Fig. S13 Comparison of the primary root parameters for three lines expressing *YFP-AtGA3ox1* from tissue-specific promoters in the *ga3ox1 ga3ox2* double mutant with those of Col-0 and the double ga3ox mutant in 7 day-old seedlings.

Fig. S14 The degree of shoot growth rescue of the *ga3ox1 ga30x2* double mutant from expressing *AtGA3ox1* from tissue-specific promoters.

Table S1 Primer sequences for amplification of cDNAs and promoters.

This article is protected by copyright. All rights reserved

Table S2 Constructs for tissue-specific expression of GA-metabolism cDNA-GFP fusions indicating the promoter expression domains in roots

Notes S1 Means, least significant differences (LSDs) and degrees of freedom (df)) for the data presented in Figures 3 – 7.

Accepted Article

This article is protected by copyright. All rights reserved

Accepted Article

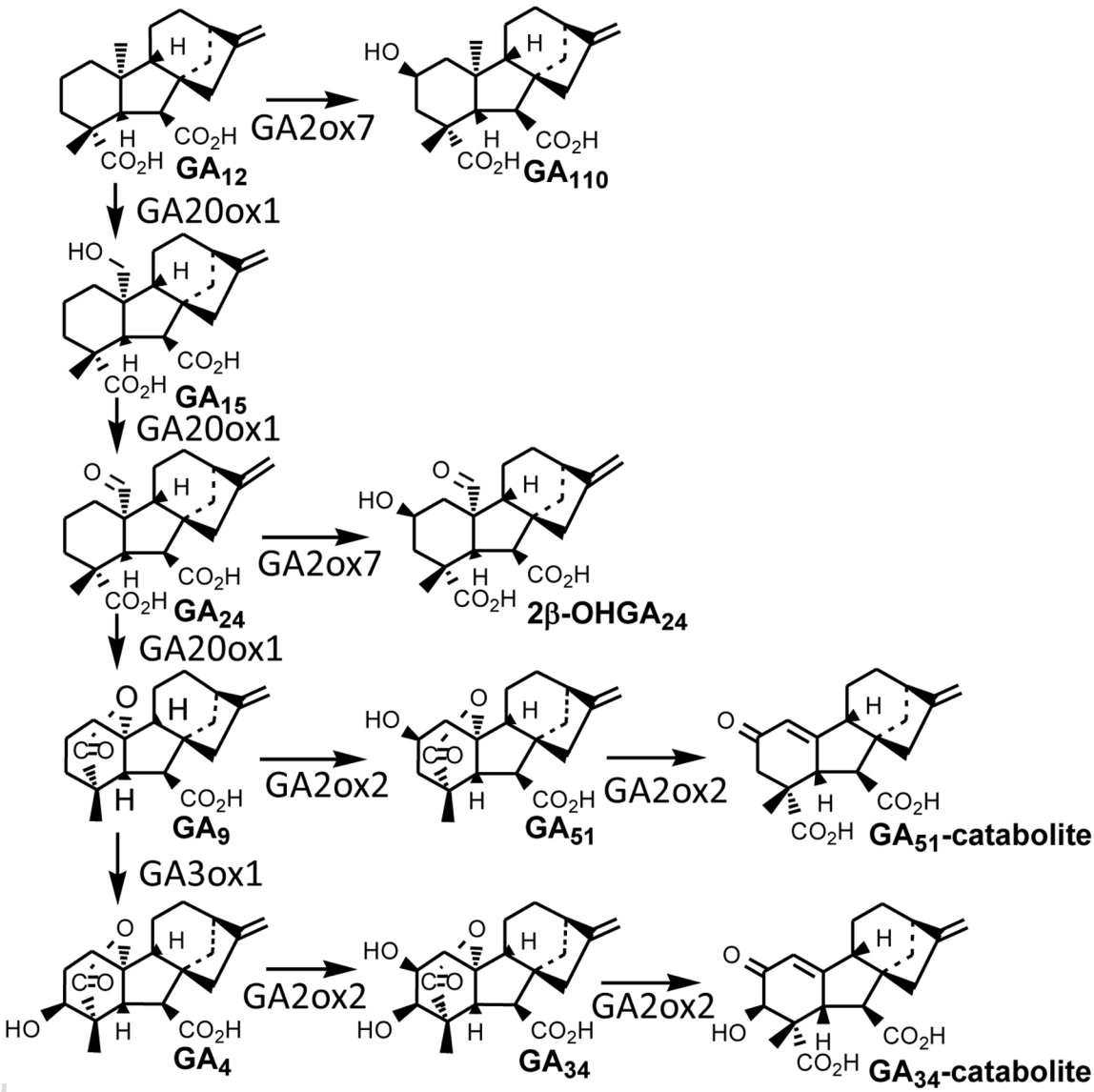

nph_16967_f1.tif

This article is protected by copyright. All rights reserved

Accepted Article

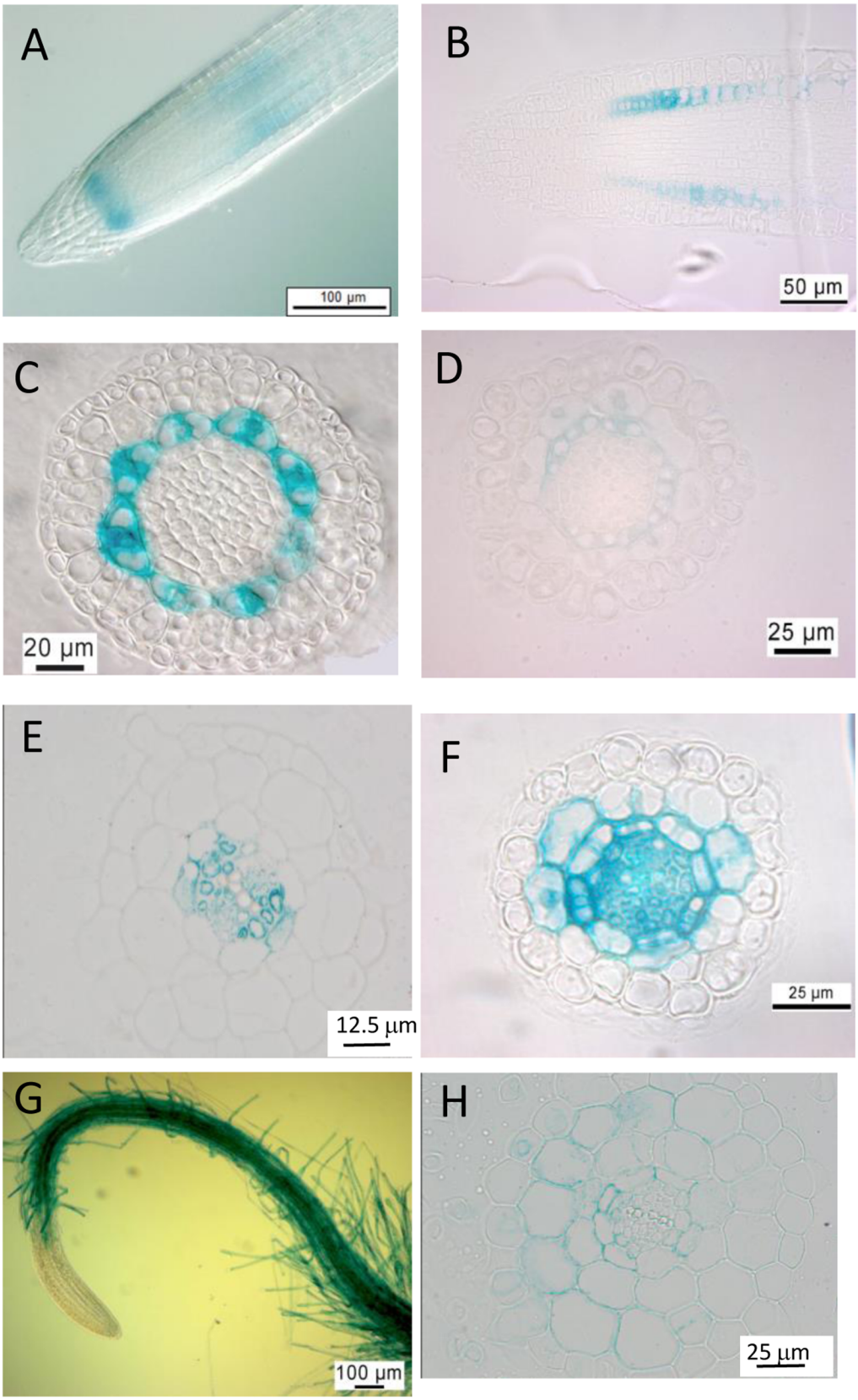

This article is protected by copyright. All rights reserved

nph_16967_f2.tif

Accepted Article

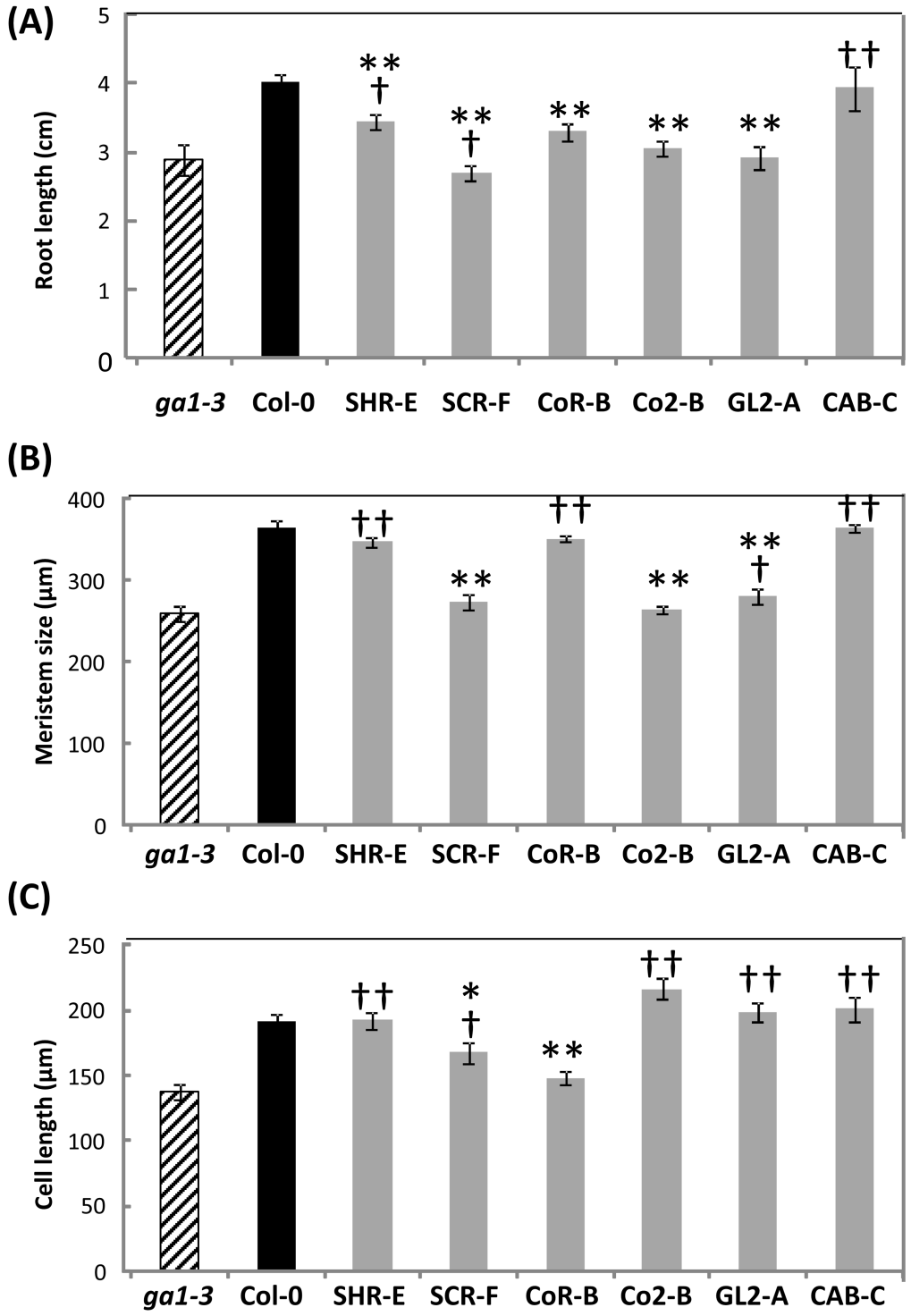

nph_16967_f3.tif

This article is protected by copyright. All rights reserved

Accepted Article

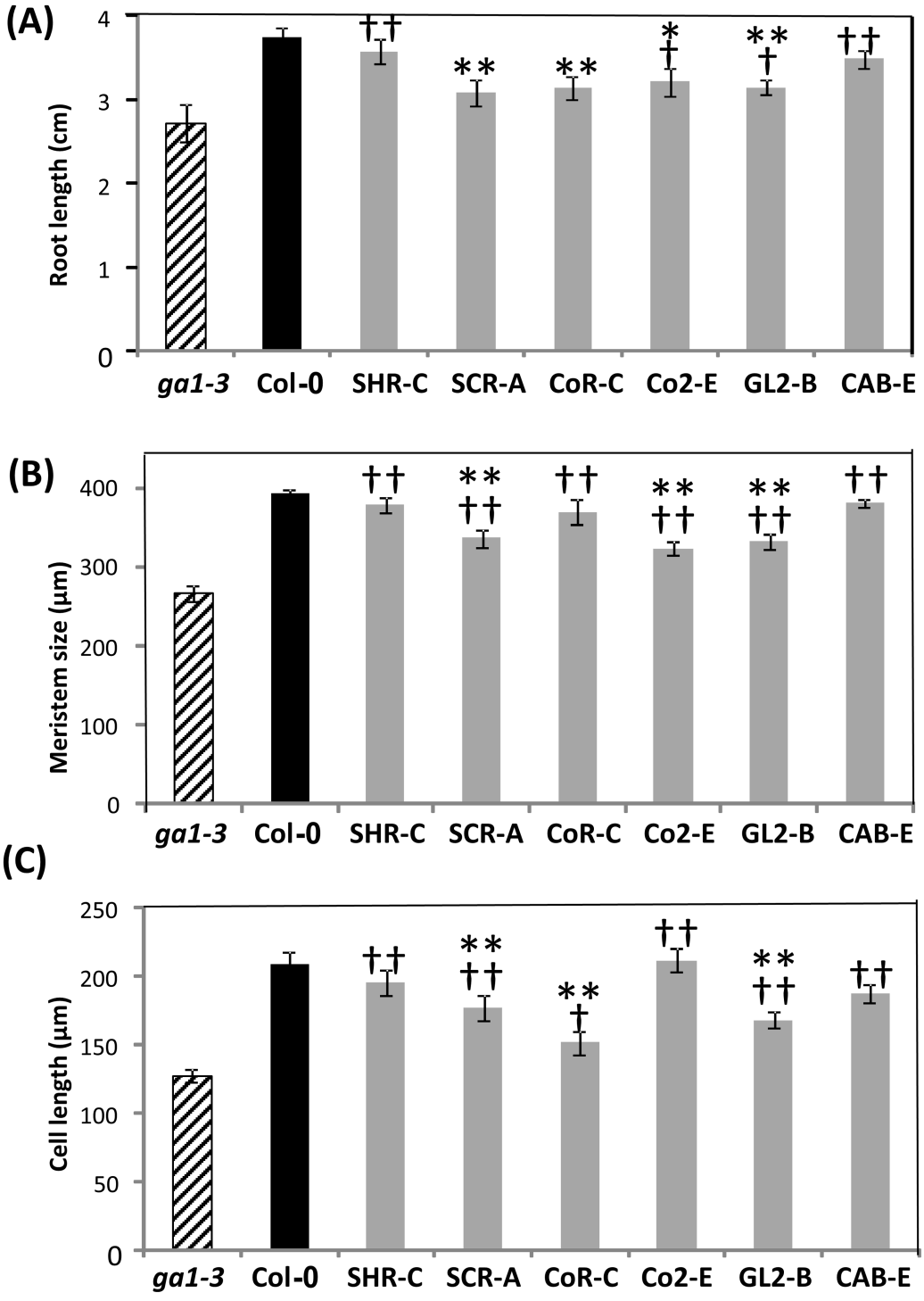

nph_16967_f4.tif

This article is protected by copyright. All rights reserved

Accepted Article

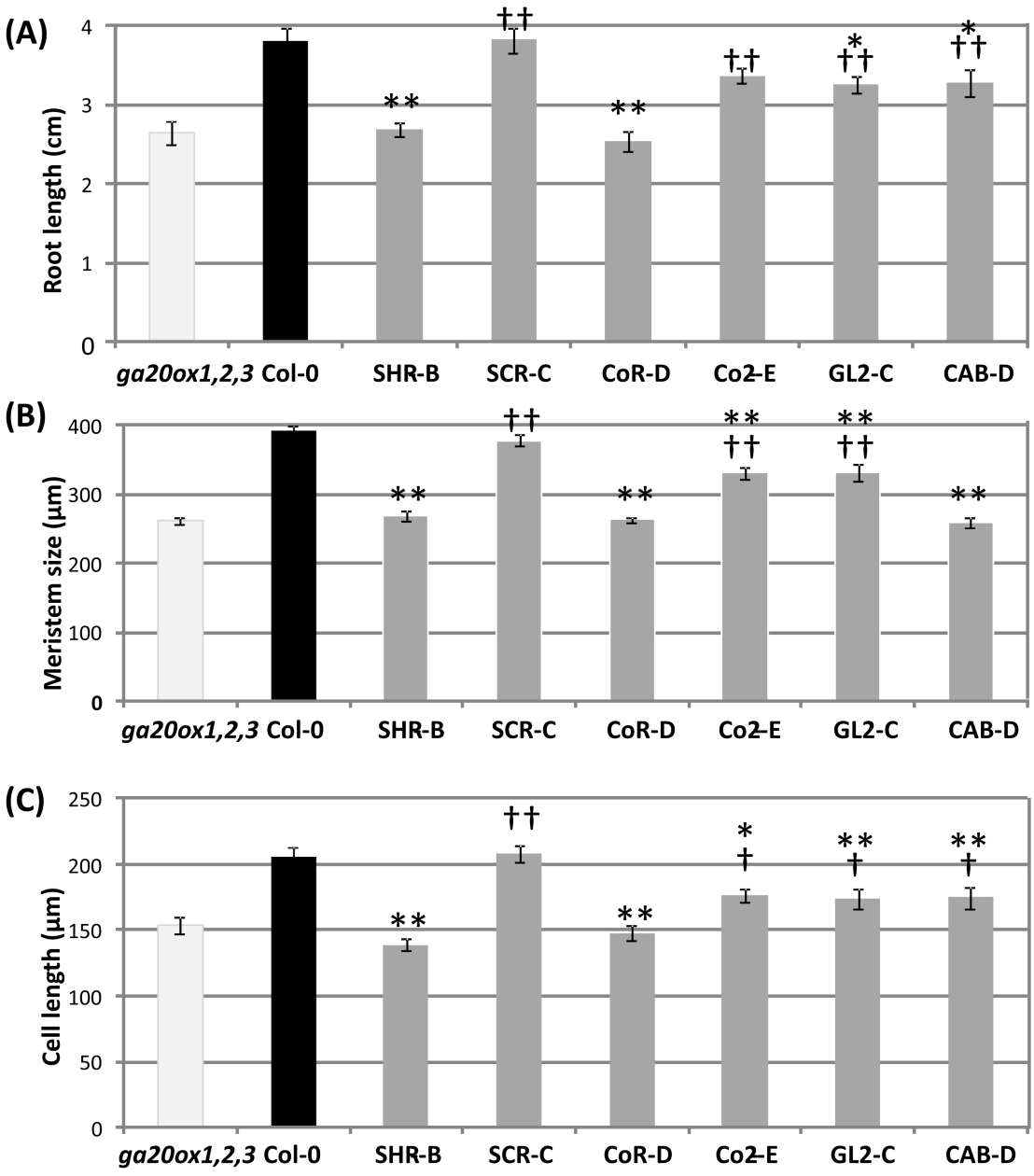

nph_16967_f5.tif

This article is protected by copyright. All rights reserved

Accepted Article

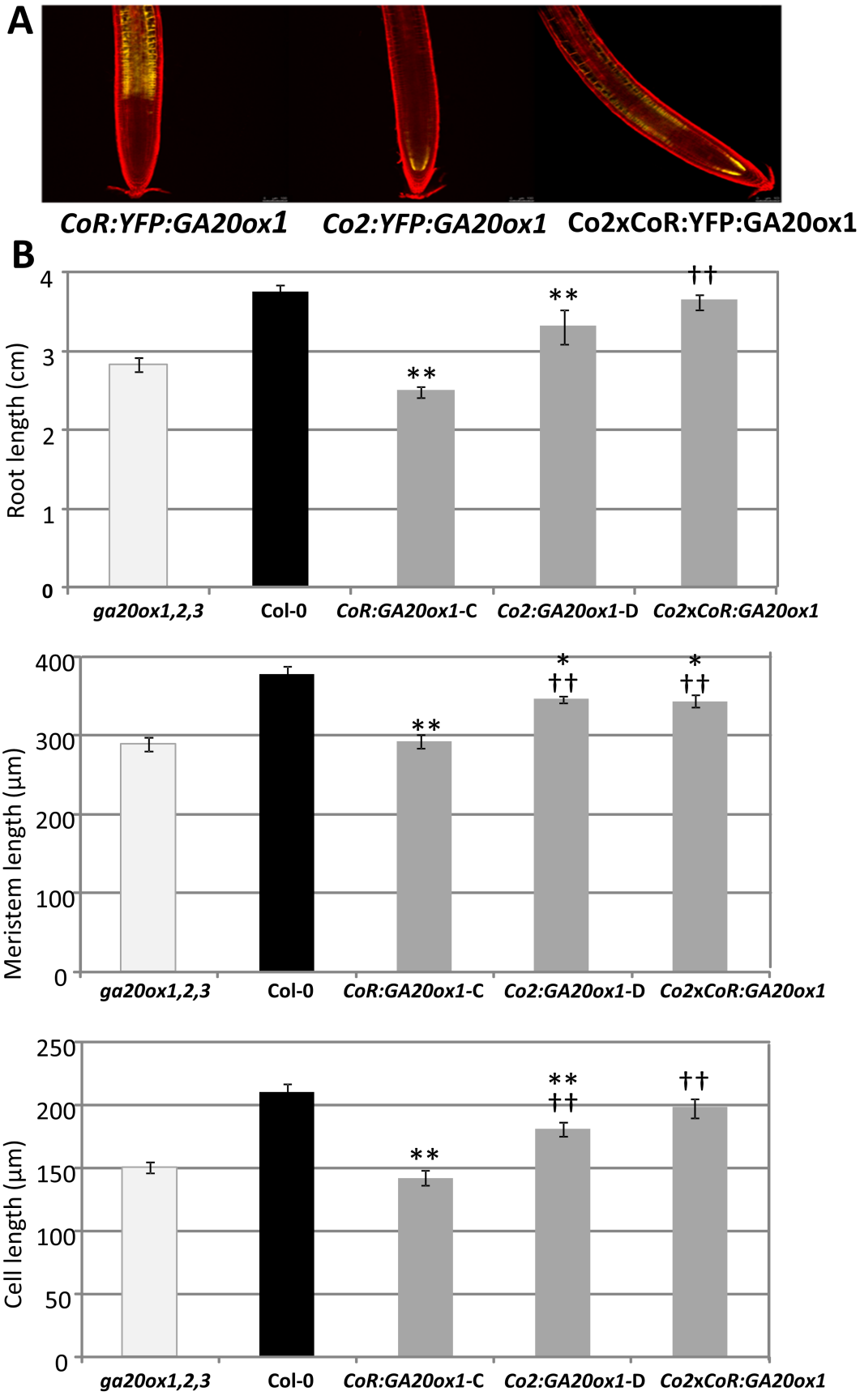

This article is protected by copyright. All rights reserved
nph_16967_f6.tif

Accepted Article

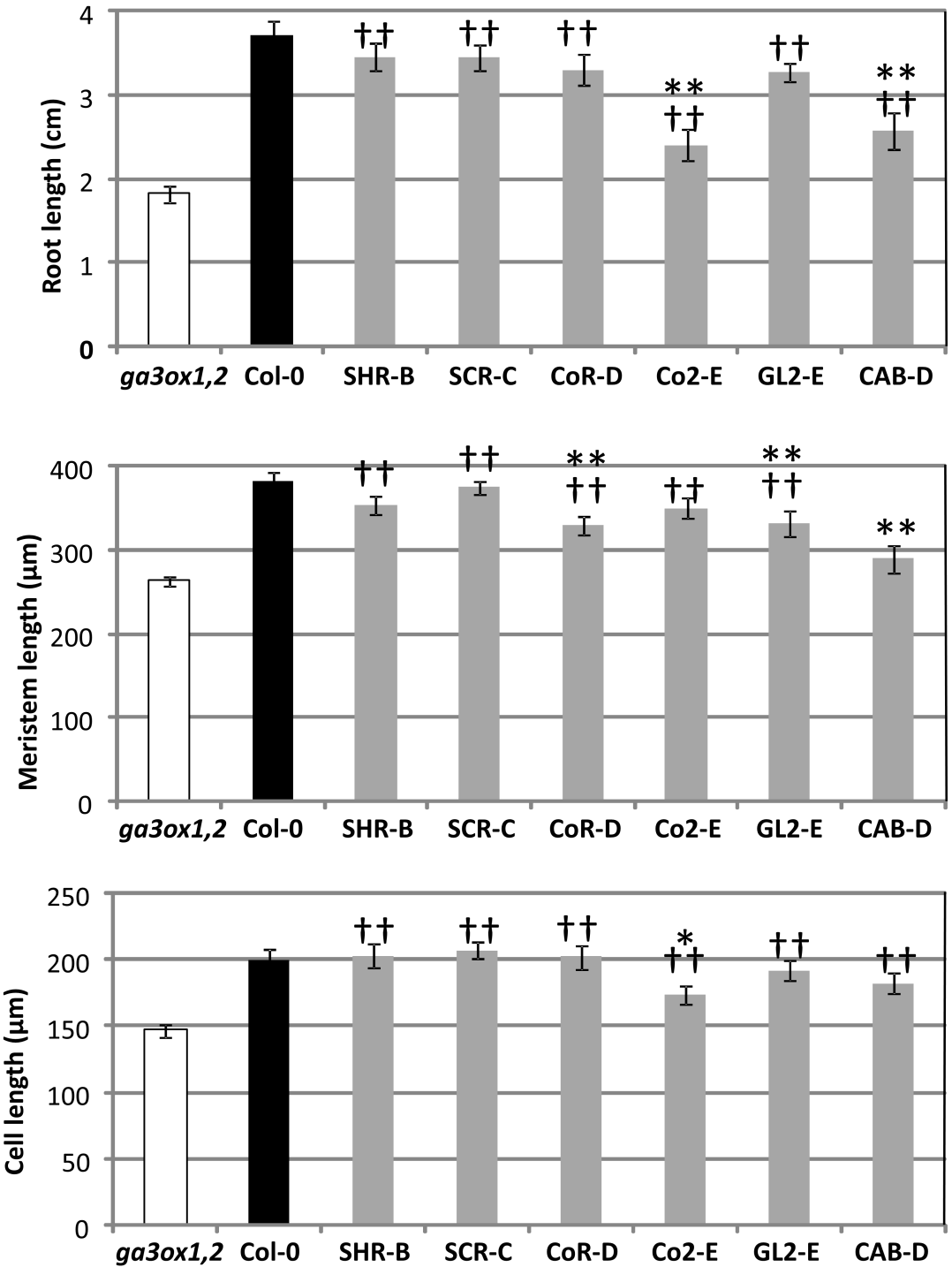

nph_16967_f7.tif

This article is protected by copyright. All rights reserved

Accepted Article

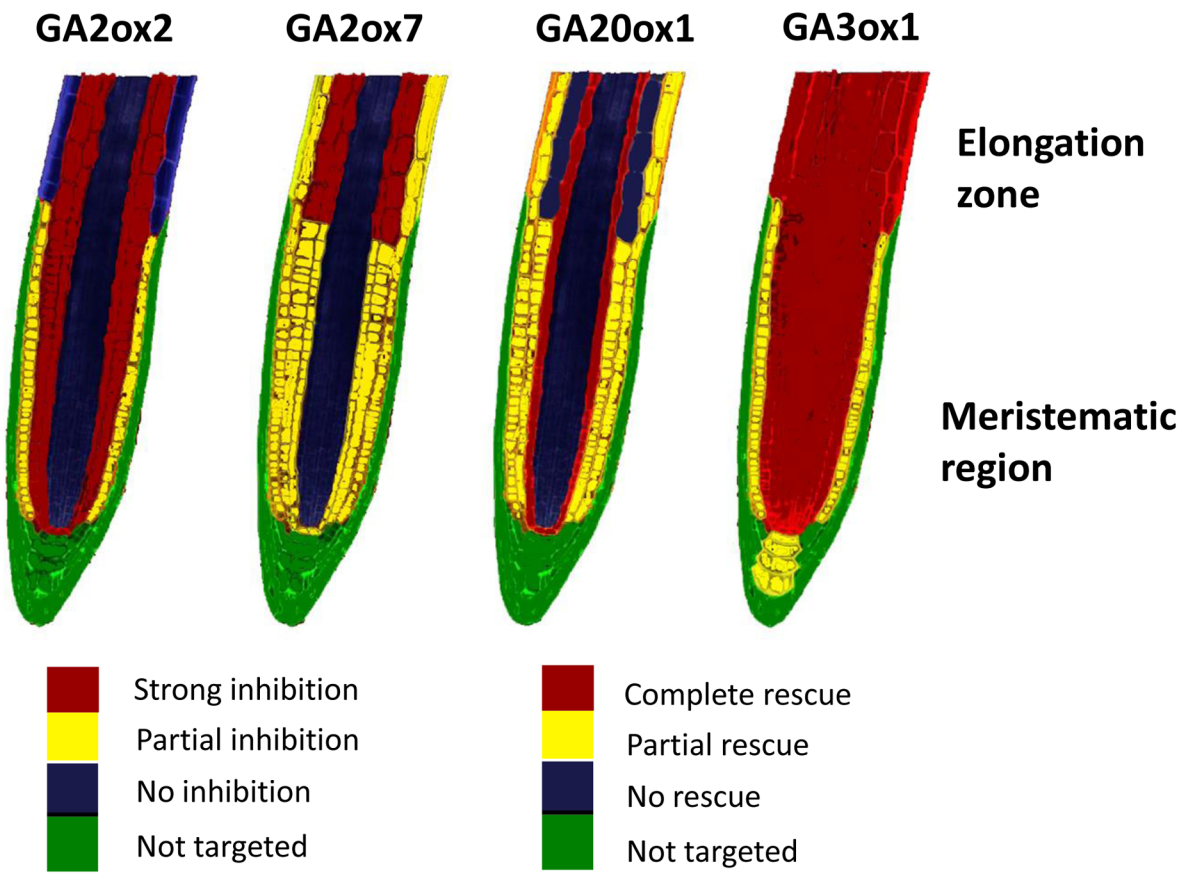

nph_16967_f8.tif

This article is protected by copyright. All rights reserved